

# Neural adaptation facilitates oscillatory responses to static inputs in a recurrent network of ON and OFF cells

Jeremie Lefebvre · Andre Longtin ·  
Victor G. LeBlanc

Received: 15 July 2010 / Revised: 6 October 2010 / Accepted: 26 November 2010 / Published online: 18 December 2010  
© Springer Science+Business Media, LLC 2010

**Abstract** We investigate the role of adaptation in a neural field model, composed of ON and OFF cells, with delayed all-to-all recurrent connections. As external spatially profiled inputs drive the network, ON cells receive inputs directly, while OFF cells receive an inverted image of the original signals. Via global and delayed inhibitory connections, these signals can cause the system to enter states of sustained oscillatory activity. We perform a bifurcation analysis of our model to elucidate how neural adaptation influences the ability of the network to exhibit oscillatory activity. We show that slow adaptation encourages input-induced rhythmic states by decreasing the Andronov–Hopf bifurcation threshold. We further determine how the feedback and adaptation together shape the resonant properties of the ON and OFF cell network and how this affects the response to time-periodic input. By introducing an additional frequency in the system, adaptation alters the resonance frequency by shifting the peaks where the response is maximal. We support these results with numerical experiments of the neural field model. Although developed in the context of the circuitry of the electric sense, these results are applicable to any network of spontaneously firing cells with global inhibitory feedback to themselves, in which a fraction of these cells receive external input directly, while the remaining ones receive an inverted version of this input via feedforward di-synaptic inhibition. Thus the results are

relevant beyond the many sensory systems where ON and OFF cells are usually identified, and provide the backbone for understanding dynamical network effects of lateral connections and various forms of ON/OFF responses.

**Keywords** Neural field · Delayed feedback · Sensory inputs · Oscillations · ON and OFF cells · Bifurcations · Frequency tuning

## 1 Introduction

The behavior of neural systems is governed by a combination of circuitry and cellular attributes. Amongst these, spike frequency adaptation is found in almost all neurons, where it is thought to influence the processing of neural information mediated by action potentials. Adaptation corresponds to a stereotyped decrease in firing rate after prolonged stimulation, as the cell habituates to steady input currents. It is thought to play a particularly important role in sensory systems. There it can alter neuronal firing patterns in order to direct the system's response towards given stimulus attributes (Benda et al. 2001; Kim and Rieke 2001; Wang et al. 2003; Gollisch and Herz 2004; Benda et al. 2005; Gabbiani and Krapp 2006) or to tune neural sensitivity to stimulus intensity (Sobel and Tank 1994). Adaptation has further been shown to control repetitive firing (Prescott et al. 2006) and influences both time and rate coding properties (Prescott and Sejnowski 2008). Various mechanisms underlying adaptation have been identified. Steady neuron firing can activate slow potassium currents (Storm 1990), which may also be calcium-dependent (Sah and Davies 2000), resulting in

---

**Action Editor: Brent Doiron**

J. Lefebvre (✉) · A. Longtin · V. G. LeBlanc  
150 Louis Pasteur, Ottawa, ON, Canada K1N 6N5  
e-mail: champvectoriel@hotmail.com

firing rate decay following a step input. Adaptation has also been linked in other cases to the inactivation of slow sodium currents (Kim and Rieke 2003). Theoretical studies on Integrate-and-Fire models as well as conductance-based models have reproduced experimental recordings of adapting behavior (see Benda et al. (2001), Liu and Wang (2001), Benda and Herz (2003) and references therein).

The goal of this paper is to investigate how adaptation shapes the frequency tuning of cells and stimulus-induced network oscillations in a realistic context of sensory feedback circuitry involving adaptive ON and OFF cells. We draw our main motivation for combining feedback, ON/OFF populations and adaptation from studies of the weakly electric fish (*Apteronotus leptorhynchus*). Adaptation has been studied there both at the level of the primary receptor known as the P-unit electroreceptor (which we do not focus on here), as well as at the level of the post-synaptic population of pyramidal cells. P-unit adaptation is very rapid (tens of milliseconds) and has been shown to influence the frequency-dependent encoding of electrosensory inputs (Xu et al. 1996; Doiron et al. 2004). This adaptation further enables the separation of fast transient stimuli, related to communication signals, from slower oscillatory signals arising from the proximity of two fish (Benda et al. 2005). This adaptation further participates in the appearance of input-induced states of synchrony (Benda et al. 2006), allowing transitions among P-units from states of synchrony to desynchrony and vice-versa due to rapid communication signals (Whittington et al. 1995). Each P-unit axon then trifurcates, with each of the three processes reaching pyramidal cells in one of three topographic maps of the electrosensory lateral line lobe (ELL). Cells especially in superficial layers of the ELL also exhibit adaptation which shapes their temporal filtering properties for oscillatory inputs that arise naturally during an encounter of two fish (Mathieson and Maler 1988; Mehaffey et al. 2008; Krahe et al. 2008). In fact adaptation becomes faster as one moves from central to lateral maps, which motivates the study here across adaptation time scales. The mechanism of this adaptation is not known but does seem to depend on calcium (Dr. Len Maler, personal communication).

It is the adaptation exhibited by these latter pyramidal cells that is of interest in our paper because they are involved in recurrent circuitry with other nuclei—as opposed to receptors which are involved only in feed-forward circuitry. In the visual system, the thalamo-cortical loop has similar properties and exhibits structures that also possess ON and OFF cells. We note that adaptation is in fact a form of negative feedback,

and as such can interact with—and even mimic—other forms of feedback caused by network circuitry. Recent dynamical studies on large scale nets have shed light on the role of adaptation in the generation and stability of spatially localized patterns like breathers (localized time-periodic bumps of activity) and traveling waves (Curtu and Ermentrout 2004; Folias and Bressloff 2005; Kilpatrick and Bressloff 2010). Other studies demonstrated its impact on network oscillations (Crook et al. 1998; Ermentrout et al. 2001; van Vreeswijk and Hansel 2001) in the form of enhanced synchronization.

Of further interest is the fact that oscillatory states can appear in sensory pathways as a consequence of sensory inputs with sufficiently high spatial coherence and/or spatial binding (Gray and Singer 1989; Borgers and Kopell 2003; Borgers et al. 2008). In the weakly electric fish such oscillations are associated with temporally random stimuli of large spatial correlation (such as other animals) and relies on delayed feedback (Doiron et al. 2003, 2004; Marinazzo et al. 2007; Lindner et al. 2005). Delayed feedback inhibition common to all cells often underlies oscillatory activity in the brain as it competes with excitatory feedback (see e.g. Pauluis et al. (1999), Pauluis (2000), Borgers and Kopell (2003), Dhamala et al. (2004), Borgers et al. (2008), Brandt and Wessel (2007) and references therein). Also, frequency tuning effects have been observed in the electric fish that change with the spatial configuration of the stimulus, i.e. on its local versus global geometry (Bastian et al. 2002; Doiron et al. 2003; Chacron et al. 2005). These are due in part to cellular and circuit properties (Chacron et al. 2005; Krahe et al. 2008). It is known for example that a step increase in stimulus contrast causes an increase followed by a decrease in ELL firing, i.e. by adaptive behavior rather than oscillatory behavior.

These studies naturally lead to the question of how adaptation interacts with spatio-temporal stimuli that lead to oscillatory dynamics. Does the presence of adaptation increase or decrease the propensity for an inhibitory recurrent network to oscillate in response to spatially correlated inputs? How does adaptation influence frequency tuning in the presence of recurrent inhibition? Cells in the ELL further display either simple ON or OFF behavior: ON (OFF) cells encode positive (negative)-going fluctuations of input signals. These signals occur as modulations of the amplitude (and sometimes frequency for communication calls) of the carrier oscillation emitted by the fish known as the electric organ discharge (EOD). ON cells (known as E cells) thus increase their firing rate when the amplitude of the EOD increases, and vice-versa for the OFF cells (known as I cells) (Berman and Maler 1998, 1999; Maler et al. 1991). The incorporation of multiple

neural populations is important to properly account for network activity and receptive field geometry and is still at the forefront of work in theoretical neuroscience (Wilson and Cowan 1972; Golomb and Ermentrout 2001; Laing and Coombes 2006; Blomquist et al. 2005). In earlier work inspired by the electrosensory circuitry, we have shown how ON and OFF populations interact with delayed and non-delayed recurrent connections to generate oscillations triggered by static stimuli (Lefebvre et al. 2009, 2010). These studies, which used neural field formulations as well as stochastic Integrate-and-Fire neurons, did not consider the issue of cellular adaptation; in fact the dynamics of networks with both multiple populations and adaptation is a general open question.

We note that the interplay of ON and OFF pathways also plays a fundamental role in vision from retina onwards (Kandel and Schwarz 1983; Gollisch and Herz 2004) as well as in audition (Robin and Royer 1987; Scholl et al. 2010) and other senses. The simple ON/OFF dichotomy described above, where each population responds preferentially to one polarity of the stimulus, is commonly present (Gabbiani 1996). Yet the circuitry and physiology, often involving many types of ON/OFF cells and complex network interactions, is far from clear and is slowly being elucidated (Gollisch and Herz 2004; Gollisch and Meister 2008; Liang and Freed 2010; Scholl et al. 2010). Here we focus on this simple type of ON/OFF behavior as opposed to other forms, such as that where both the onset and offset of a stimulus both cause firing rate increases (Scholl et al. 2010) (in the simple dichotomy illustrated above, ON and OFF populations would have inverted responses with respect to one another for both onset and offset).

In contrast, ON/OFF circuitry (known as E/I circuitry) has been worked out for weakly electric fish, and can be summarized as follows: ON and OFF cells share common P-unit afferents, but the OFF pathway includes an interposed inhibitory interneuron, causing the OFF response to be inverted (Berman and Maler 1998, 1999). Electrosensory thus offers a relatively simpler sensory system, both anatomically and physiologically, in which to investigate the role of adaptive ON/OFF cells involved in recurrent circuitry. Such a study can then provide the dynamical backbone for more complex systems and forms of ON/OFF responses. It is important to note that earlier modeling studies of oscillations in ELL assumed only one population was at work (the ON population (Doiron et al. 2003, 2004; Marinazzo et al. 2007; Lindner et al. 2005)).

In this paper, we address the following questions: how does adaptation influence the oscillatory response threshold in networks of ON and OFF cells? Are global

oscillations as common when adaptation is included? How does the combination of adaptation and feedback shape frequency tuning of cells embedded in the network? Our work here builds on our previous results about ON and OFF cells and delayed feedback without adaptation. We investigate how adaptation may underlie stimulus-induced oscillations in recurrent networks. To demonstrate this, we compare the Andronov–Hopf bifurcation scenario for the cases with and without adaptation. We thus expand the stability analysis around steady activity states in a recurrent model that now includes adaptation dynamics. We will highlight the effect of adaptation on the stability of input-induced limit cycles. We will also study how such a model responds to time-periodic input, and how adaptation shapes the resonance curve by introducing additional time-scales in the system.

In Section 2, we describe the architecture of our ON/OFF network and we show how stable oscillations appear as a result of spatially localized stimulation. In Section 3, we perform a stability analysis of our model, incorporating adaptation, where we compare the instability point between the cases where adaptation is and is not present. There, our study has been made more analytically tractable by assuming identical adaptation dynamics for the ON and OFF cells. We further look at the impact of adaptation on the system's steady states, to determine how external input then interact with the feedback. Lastly, in Section 4, we investigate and compare the effects of adaptation and feedback on the amplitude of the cells response to time-varying inputs. We further motivate those results by comparing the resonance curves with those obtained with a noisy Integrate-and-Fire net.

## 2 Model

Our model is based on electroreception, but is general enough to apply to other senses (Fig. 1). We describe the evolution of the neural activity  $u(x, t)$ , corresponding to the mean somatic membrane potential of a sub-network of the whole network located at position  $x$  along a one-dimensional spatial domain  $\Omega$ . This activity is further segregated into that of ON and OFF populations  $u_{on,off}$ . External sensory signals  $I(x, t)$  propagate in a parallel fashion from the first receptors (not modeled explicitly) up to the “sensory” layer of pyramidal cells in the ELL, and excite and/or inhibit the local populations by altering their activity level. Further, recurrent connections allow the activity of the cells to propagate to higher brain centers (mainly area NP in the weakly electric fish (Berman and Maler 1999)).

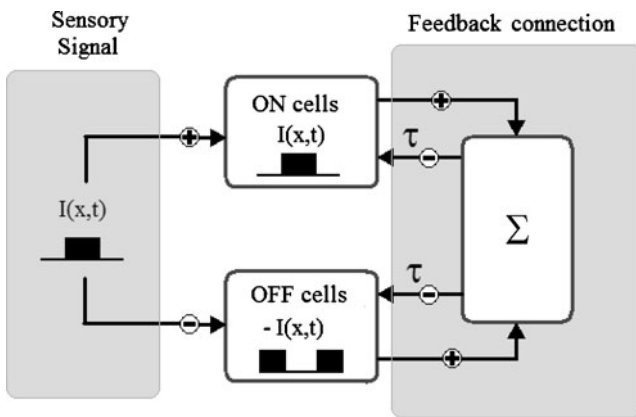


**Fig. 1** Network architecture of our model. It is inspired from the ELL of the weakly electric fish. The sensory layer, built of an equal number of ON and OFF cells, receives external sensory inputs with direct (ON) and inverted (OFF) polarity. The populations then project to higher centers, which accumulate the activity distributed across the network (*sigma* symbol). The recurrent connections allows the accumulated activity component to be sent back to all the cells in the sensory layer with some time lag  $\tau$

For simplicity the activity there is summed across the network and then fed back to all the initial sites globally and with inhibitory polarity. This component of the circuit involves a significant processing and propagation time lag modeled with a fixed delay  $\tau$ . The fields  $u_{on}$  and  $u_{off}$  obey the dynamics

$$\begin{aligned} (1 + a^{-1} \partial_t) u_{on}(x, t) &= -A(t - \tau) + I(x, t) \\ (1 + a^{-1} \partial_t) u_{off}(x, t) &= -A(t - \tau) - I(x, t), \end{aligned} \quad (1)$$

where  $a$  is the rate constant of the exponential synapses with response function  $\eta(t) = ae^{-at}$ , and  $A$  is the delayed inhibitory feedback connection, corresponding to the accumulation of activity of each unit across the network:

$$\begin{aligned} A(t - \tau) &= \int_{\Omega} dy [\alpha_{on} f(u_{on}(y, t - \tau)) + \alpha_{off} f(u_{off}(y, t - \tau))]. \end{aligned}$$

Here,  $\alpha_{on}$  and  $\alpha_{off}$  are the relative proportions of ON and OFF cells in the network, which have been both set to 0.5. The function  $f$  is a sigmoidal firing rate function defined by  $f(u) = (1 + \exp(-\beta(u - h)))^{-1}$  for a gain of  $\beta$  and an activation threshold  $h$ . The feedback gain  $\beta$  is fixed to 25 throughout the analysis.

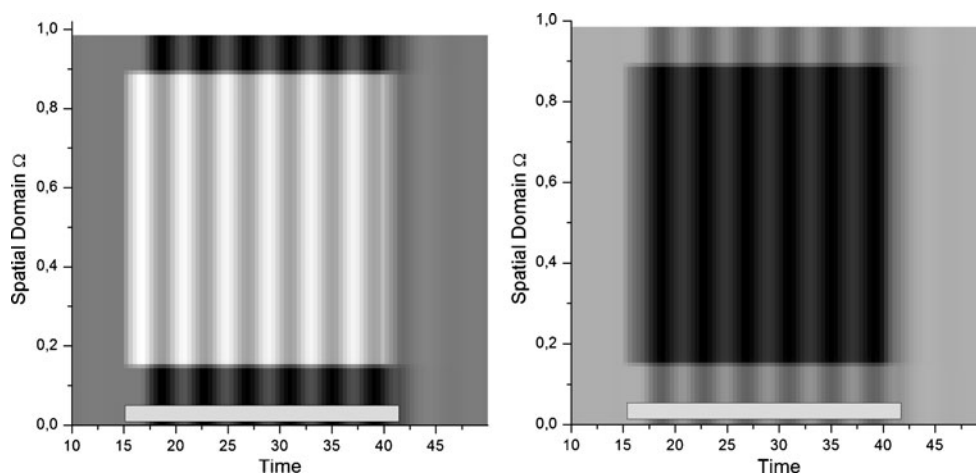
The ELL in the weakly electric fish exhibits a similar architecture to the one used in this model. Indeed, very few lateral connections exist within it, such that most

of the processing is performed by the means of feedback connections from higher nuclei. Previous studies (Lefebvre et al. 2009, 2010) demonstrated that this model exhibits changes from stable activity equilibria to global oscillations as a result of increasing stimulus amplitude and/or spatial extent, due to the presence of an Andronov–Hopf bifurcation. Those neural field predictions were further supported by simulations of a network of noisy Integrate-and-Fire neurons with spatio-temporal forcing, as in Lindner et al. (2005) and Doiron et al. (2003, 2004) for the case where only ON cells were considered. Weaker effects of local non-delayed circuitry within the ELL itself have also been studied (Lefebvre et al. 2010), and were shown to be of no qualitative consequence on the dynamics; such local effects are thus not modeled here.

Aside from their inhibitory response to positive inputs, OFF cells in-vivo can fire at a baseline mean rate even in absence of external stimulation, as may ON cells (Robin and Royer 1987; Laing and Coombes 2006). In the electric sense, both ON and OFF cells are spontaneously active because they receive tonic excitation from various sources. Thus, external input modulates the firing activity of both ON and OFF cells around this baseline activity. Experimental recordings in the electrosensory system indicate that the spontaneous firing rate may even be slightly higher for OFF cells than for ON cells. Our recent results, in the context where no adaptation is present, demonstrate that such a significant difference in spontaneous activity between these neural populations can qualitatively alter the input response of ON/OFF nets (Laing and Coombes 2006). While the inclusion of this activity difference in our network with adaptation is easy to do (e.g. by adding a bias current to one neuron population) and would further enhance the connection of our results with the physiology of real ON/OFF systems, the analysis would become much more complicated as a function of this asymmetry. Thus, for simplicity, we assume throughout that both neural populations share the same baseline activity in the absence of input. This allows us to focus more clearly on the influence of adaptation on the resonance and oscillatory properties of such nets. Also, our results are generally applicable to any network of spontaneously firing cells with global inhibitory feedback to themselves, in which a fraction of these cells receive external input directly, while the remaining ones receive an inverted version of this input via feedforward di-synaptic inhibition.

Without adaptation, observed global oscillations can emerge as network responses to spatially distributed signals. Figure 2 shows the response of ON and OFF populations to an input of the form  $I(x, t) = I_0 \neq 0$

**Fig. 2** Oscillatory response of ON (*left panel*) and OFF (*right panel*) populations to a spatially localized pulse. Parameters are  $a = 1$ ,  $\tau = 1.4$ ,  $h = 0.1$  and  $\Omega = [0, 1]$ . The input has an amplitude  $I_o = 0.3$  and possess a spatial width  $\Delta \equiv |x_2 - x_1| = 0.75$  where  $x_1 = 0.15$  and  $x_2 = 0.90$  and for  $15 < t < 40$



if  $x_1 < x < x_2$  and  $t_1 < t < t_2$  (and  $I = 0$  otherwise). The stimulus triggers a global oscillatory response by causing an Andronov–Hopf bifurcation, for which the details have already been worked out (Lefebvre et al. 2009). The linearization and subsequent eigenvalue analysis of system (1) for spatially homogeneous eigenmodes of the form  $u_j(x, t) = \bar{u}_j(x) + \tilde{u}e^{\lambda t}$  for  $\tilde{u}, \in \mathbb{R}, \lambda \in \mathbb{C}$ , yields the characteristic equation

$$\lambda + 1 + Re^{\lambda\tau} = 0, \tag{2}$$

for  $R = \frac{1}{2}[\int_{\Omega} dyf'(\bar{u}_{on}(y)) + \int_{\Omega} dyf'(\bar{u}_{off}(y))]$ . The case with adaptation is more involved, as we show next.

### 3 Neural adaptation

While the idealized network architecture of Eq. (1) allows the cellular populations to maintain a steady (or oscillating) level of activity, more realistic network descriptions typically include *adaptation*. As we will see, this local intrinsic component of cellular dynamics plays a crucial role in balancing the excitation-inhibition ratio across the system. It is therefore an important factor to consider in the genesis of global oscillations as well as possible resonance effects. Various biophysical mechanisms have been shown to cause adaptation, generating distinct effects on the spiking dynamics (Benda and Herz 2003; Ermentrout et al. 2001; Prescott and Sejnowski 2008; Benda et al. 2010). Here we incorporate an intrinsic linear adaptation that is modeled as a second field, acting locally and subtractively on the activity field (1). Note that we are not modeling a specific outward current. Rather, this adaptation field can be seen as a subtractive current that approximates the impact of a number of realistic adaptation mech-

anisms on firing rate and resonance properties. This model adaptation field will thus reflect the effect of this linear component on the evolution of spatio-temporal activity. Our model now becomes:

$$\begin{aligned} (1 + a^{-1}\partial_t) u_{on}(x, t) &= -A(t - \tau) + I(x, t) \\ &\quad - \epsilon_{on}w_{on}(x, t) \\ (1 + a^{-1}\partial_t) u_{off}(x, t) &= -A(t - \tau) - I(x, t) \\ &\quad - \epsilon_{off}w_{off}(x, t), \end{aligned} \tag{3}$$

where the adaptation fields  $w_{on,off}(x, t)$  obey

$$\begin{aligned} (1 + b^{-1}\partial_t) w_{on}(x, t) &= u_{on}(x, t) \\ (1 + b^{-1}\partial_t) w_{off}(x, t) &= u_{off}(x, t). \end{aligned} \tag{4}$$

Here  $b$  is the rate of the adaptation ( $b^{-1}$  is the adaptation time constant) and  $\epsilon_{on,off} > 0$  corresponds to the gain or amplitude of the adaptation component, which acts as an inhibitory feedback. System (3) includes two additive inhibitory components which obey linear dynamics and operate on the time scale  $b^{-1}$ , which we assume is identical for ON and OFF cells. Further, the adaptation gain is assumed to be identical for both ON and OFF cells i.e.  $\epsilon_{on} = \epsilon_{off} = \epsilon$ . The fields  $w_{on,off}(x, t)$  are expected to locally inhibit the activity of both ON or OFF populations whenever the ON and OFF activities  $u_{on,off}(x, t)$  increase. The instability threshold for which global oscillations can be triggered by static local stimuli will change according to the gain and relative time scale of this new inhibitory mechanism.

To determine the impact of adaptation, one needs to rework the stability analysis taking into account the

increased dimensionality of the problem. This analysis relies on the symmetry between ON and OFF cells and is restricted to the choice of identical adaptation gains and time scales for both sub-populations. The steady states of the combined systems (3) and (4) are solutions of:

$$(1 + \epsilon)\bar{u}_{on}(x) = -A(\bar{u}_{on}, \bar{u}_{off}) + I(x)$$

$$(1 + \epsilon)\bar{u}_{off}(x) = (1 + \epsilon)\bar{u}_{on}(x) - 2I(x), \quad (5)$$

where  $\bar{w}_{on} = \bar{u}_{on}(x)$  and  $\bar{w}_{off} = \bar{u}_{off}(x)$ . Adaptation acts as a contracting components, reducing the amplitude of the steady states by a factor  $(1 + \epsilon_{on,off}) > 0$ . Considering the spatially homogeneous eigenmodes  $u_j(x, t) = \bar{u}_j(x) + \bar{u}e^{\lambda t}$  and  $w_j(x, t) = \bar{w}_j(x) +$

$\bar{w}e^{\lambda t}$ ,  $\bar{u}, \bar{w} \in \mathbb{R}, \lambda \in \mathbb{C}$ , one obtains from Eqs. (3) and (4) the Jacobian with delayed components

$$\mathbb{J}(\lambda) = \begin{pmatrix} -a(1 + R_{on}(\bar{u}_{on})e^{-\lambda\tau}) & -aR_{off}(\bar{u}_{off})e^{-\lambda\tau} & -a\epsilon & 0 \\ -aR_{on}(\bar{u}_{on})e^{-\lambda\tau} & -a(1 + R_{off}(\bar{u}_{off})e^{-\lambda\tau}) & 0 & -a\epsilon \\ b & 0 & -b & 0 \\ 0 & b & 0 & -b \end{pmatrix}$$

$R_{on} = \frac{1}{2}[\int_{\Omega} dy f'(\bar{u}_{on}(y))]$  and  $R_{off} = \frac{1}{2}[\int_{\Omega} dy f'(\bar{u}_{off}(y))]$ . The characteristic equation follows as

$$0 = \det(\mathbb{J}(\lambda) - \lambda\mathbb{I}_4), \quad (6)$$

with  $\mathbb{I}_4$  being the  $4 \times 4$  identity matrix. The resulting fourth-order polynomial in  $\lambda$  admits the following solutions

$$\lambda_{1,2} = -\frac{a+b}{2} \pm \frac{1}{2}\sqrt{b^2 - 2ab + a^2 - 4ab\epsilon},$$

$$\lambda_{3,4} = -\frac{aRe^{-i\omega\tau} + a + b}{2}$$

$$\pm \frac{1}{2}\sqrt{(Rae^{-\lambda\tau})^2 + 2a^2Re^{-\lambda\tau} - 2abRe^{-\lambda\tau} + a^2 - 2ab + b^2 - 4ab\epsilon}, \quad (7)$$

where the eigenvalues  $\lambda_{3,4}$  are implicitly determined. The function  $R$  can be expressed as

$$R = R_{on}(\bar{u}_{on}) + R_{off}(\bar{u}_{off})$$

$$= \frac{1}{2} \left[ \int_{\Omega} dy f'(\bar{u}_{on}(y)) \right] + \frac{1}{2} \left[ \int_{\Omega} dy f'(\bar{u}_{off}(y)) \right]. \quad (8)$$

The eigenvalues  $\lambda_{1,2}$  define the stability of Eq. (4) and thus do not depend on the delay  $\tau$ . Given that  $a, b, \epsilon > 0$ ,  $\lambda_{1,2}$  remain bounded to the left of the imaginary axis and subsequently do not contribute to any oscillatory instability. They however introduce an additional frequency in the system, whenever  $\lambda_{1,2} \in \mathbb{C}$  with non-zero imaginary parts. An input-induced oscillation requires the non-linear delayed feedback connections. We may therefore restrict the analysis to the eigenvalues  $\lambda_{3,4}$ , which depend on the delay  $\tau$  as well as the parameter  $R$ . At the instability threshold,  $\lambda_{3,4} = \{iw_k | \mathbb{R} \ni w_k > 0\}$ , and we obtain the same criterion for an Andronov–Hopf bifurcation from both  $\lambda_3$  and  $\lambda_4$ , namely

$$0 = (2iw + aRe^{-i\omega\tau} + a + b)^2 - a^2 - 2a^2Re^{-i\omega\tau}$$

$$+ 2ab - R^2a^2e^{-2i\omega\tau} + 2abRe^{-i\omega\tau} - b^2 + 4ab\epsilon. \quad (9)$$

Expanding and separating the real and imaginary components using  $e^{-i\omega\tau} = \cos(\omega\tau) - i\sin(\omega\tau)$ , we obtain

$$0 = -w^2 + awR \sin(\omega\tau) + ab(\epsilon + 1) + abR \cos(\omega\tau)$$

$$0 = awR \cos(\omega\tau) + (a + b)w - abR \sin(\omega\tau), \quad (10)$$

Combining these equations, the instability threshold  $R_c$  becomes

$$R_c \cos(\omega(R_c)\tau) = -\frac{b^2(\epsilon + 1) + w(R_c)^2}{b^2 + w(R_c)^2}, \quad (11)$$

for which the frequencies can be shown to be

$$\omega(R_c, \epsilon, a, b)$$

$$= \pm \frac{1}{2} * \sqrt{P_1(R_c, \epsilon, a, b) \pm 2\sqrt{P_2(R_c, \epsilon, a, b)}},$$

with the polynomials

$$P_1(R_c, \epsilon, a, b) = 2(R_c^2 - 1)a^2 - 2b^2 + 4ab\epsilon,$$

$$P_2(R_c, \epsilon, a, b) = b^4 - 4b^3a\epsilon - 2a^2b^2$$

$$+ 2R_c^2a^2b^2 - 4a^3b\epsilon + 4a^3b\epsilon R_c^2$$

$$+ a^4 - 2a^4R_c^2 + R_c^4a^4 - 8b^2a^2\epsilon.$$

Equation (11) defines the instability threshold as a function of the adaptation gain  $\epsilon$  and time scale  $b^{-1}$ . The reader might notice that whenever  $\epsilon, b = 0$ , one recovers the eigenvalue problem exposed in Eq. (2), in which no adaptation was present.

The problem of determining the overall effect of cellular adaptation on input-induced oscillations is twofold. First, one must see how  $\epsilon > 0$  and  $b > 0$  change the value of the instability threshold  $R_c$  in Eq. (11) with respect to the case without adaptation i.e.  $\epsilon = 0, b = 0$ . Secondly, one must see whether  $\epsilon > 0$  reshapes the function  $R$  in Eq. (8) by shifting the steady states. Thus, we must consider the fact that adaptation might not only change the critical value  $R_c$  where an oscillatory response occurs, but also the trajectory in parameter space on which the system reaches stable cyclic solutions.

Figure 3 exposes the effect of increasing gain and adaptation rate constant on the instability threshold  $R_c$  in Eq. (11). For  $b$  small,  $R(b, \epsilon) < R_c$ . The Andronov–Hopf threshold becomes smaller as the gain increases  $\epsilon > 0$ , meaning that oscillatory states require weaker inputs to be reached. As  $b$  increases, the opposite occurs, and the threshold increases away from the case  $\epsilon = 0$ . Cellular adaptation in the electrosensory system operates on time scales of roughly 100ms, slower than the intrinsic dynamics of the cells, which are on the order of 10–20 ms (Krahe et al. 2008). As a result,  $b$  is

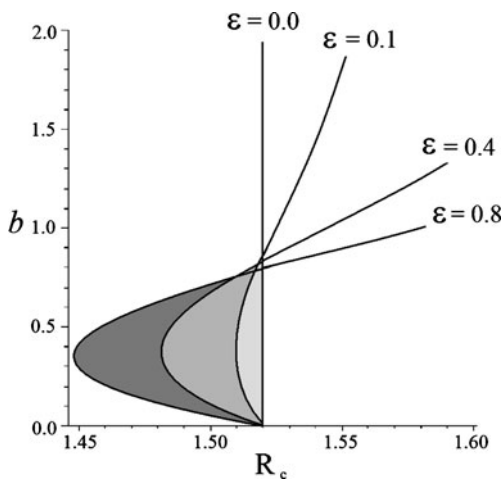


**Fig. 3** Oscillatory response threshold  $R_c$  as a function of the adaptation gain  $\epsilon$  and time constant  $b^{-1}$ . Slow adaptation ( $b$  small) reduces the response threshold marginally, while on faster time scales, the threshold is increased, reducing the tendency of the system to enter oscillatory states of activity in response to static stimuli. The adaptation gain  $\epsilon$  amplifies both effects. We note that for  $b \approx 0.8$ , the gain  $\epsilon$  has almost no effect on the value of  $R_c$ . Parameters are  $a = 1, \tau = 2.0, \alpha_{on,off} = 0.5$  and  $\Omega = [0, 1]$

more likely to be smaller than the cellular rate constant  $a$ , here fixed to  $a = 1$ . For this interval of  $b$  values, slow adaptation enhances the prevalence oscillatory responses by reducing the value of the bifurcation threshold.

The effect of local stimulation on the function  $R$  for  $\epsilon = 0$  has been investigated (Lefebvre et al. 2009), but additional inhibitory components like adaptation influence the steady states as well. Indeed, from Eq. (5) and by considering the weak feedback regime i.e.  $f(\bar{u}_{on,off}) \approx 0$ , adaptation reduces the response contrast by a factor  $(1 + \epsilon_{on,off})^{-1}$ . Figure 4 shows the response amplitude of stimulated cells as a function of the adaptation gain  $\epsilon$ . The input contrast is defined by the activity difference between stimulated and non-stimulated sites for networks with  $\epsilon = 0$  and  $\epsilon > 0$  in the steady state regime. This definition refers to the dynamics out of any oscillatory regimes and is used to specify the net impact of inputs on the activity of the sub-units. Once oscillations appear, we use the term “response” instead to qualify the magnitude of the oscillations (see Section 4). As the adaptation gain increases, the response amplitude decreases. As a result, the amplitude of the inhibitory feedback for  $\epsilon > 0$  is smaller than for  $\epsilon = 0$ ; this allows the steady states to

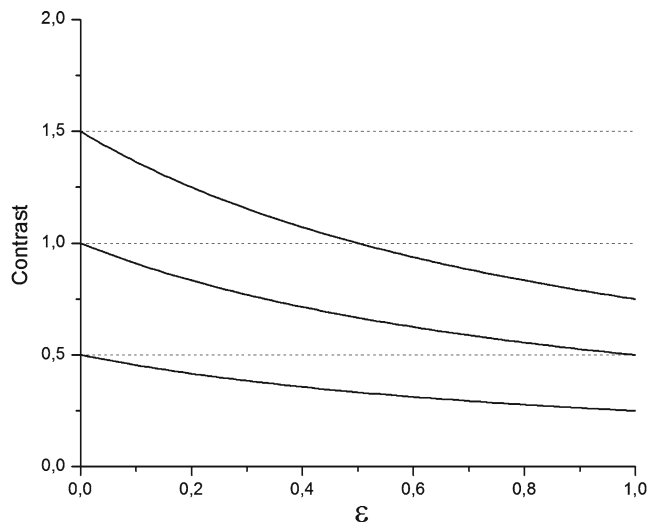


**Fig. 4** Input contrast for a static pulse of the form  $I(x, t) = I_o$  if  $x \in \Delta$  and  $t_1 < t < t_2$  where  $\Delta$  corresponds to the input spatial width, defined by  $\Delta = |x_1 - x_2|$ . The contrast is the difference in activity of units inside and outside the pulse. As the adaptation gain increases, the local response decreases. The activity levels have been chosen such that the feedback connections are weakly interacting with the ON and OFF population activities. The solid curves illustrate the contrast when adaptation is present and as a function of the gain  $\epsilon$  for different input amplitudes, while the dashed lines show the response for  $\epsilon = 0$

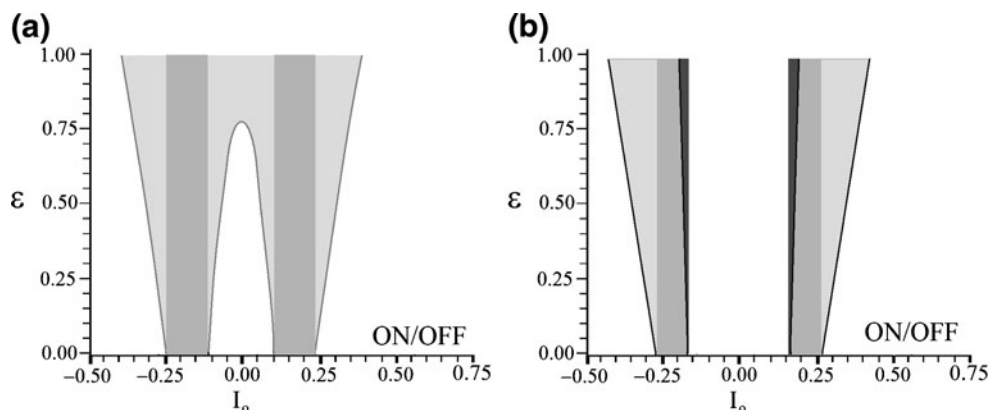


**Fig. 5** Points in  $(I_o, \epsilon)$  parameter space for which an Andronov–Hopf bifurcation occurs. The input is a stationary pulse as in Fig. 4 for a fixed width. **(a)** Due to the presence of ON and OFF cells, oscillatory responses are observed for both excitatory ( $I_o > 0$ ) and inhibitory ( $I_o < 0$ ) pulses, making the functional  $R(I_o, \epsilon)$  symmetric with respect to  $I_o$ , irrespective of the spatial extent of the stimulus. Because  $h$  is small ( $h = 0.07$ ), as  $\epsilon$  increases, the minimal input amplitude causing an Andronov–Hopf bifurcation is smaller, enhancing the tendency of the system towards cyclic

activity, and the interval of values broadens. The vertical dark gray bands correspond to the case without adaptation ( $\epsilon = 0$ ). **(b)** For larger feedback thresholds (i.e.  $h = 0.1$ ), the mean value of the function  $R(I_o, \epsilon)$  is smaller for  $\epsilon > 0$ . The minimal input amplitude causing an Andronov–Hopf bifurcation becomes larger as  $\epsilon$  increases. Here, the feedback threshold is  $h = 0.1$ . Parameters are  $a = 1$ ,  $\tau = 2.0$ ,  $\Omega = [0, 1]$ . The pulse width is  $\Delta = 0.5$ . The rate constant  $b$  was set to 0.8, where the critical value  $R_c$  remains approximately constant as  $\epsilon$  changes (see Fig. 3)

reach higher values. This can be verified numerically by solving Eq. (5) for both  $\epsilon > 0$  and  $\epsilon = 0$ , or analytically by considering only the first Taylor expansion term of  $f$ .

Adaptation also reduces the magnitude of the feedback signal sent to the sensory layer in the same way that it limits the response contrast. Even though the same amount of feedback connections gets recruited, the amplitude of the return signal is reduced; the amount of inhibition in the system decreases. As such, increasing the adaptation gain does in part increase the activity of the ON and OFF populations. The behavior of the system with respect to stimulation is a trade-off between a weaker contrast and inhibition. As a consequence, this modification of the steady states significantly alters the way the system interacts with the non-linearities of Eq. (1) and thus changes the location in parameter space where a bifurcation occurs. To understand this effect, we need to investigate the consequences of  $\epsilon > 0$  on the shape of the function  $R = R(\epsilon)$  in Eq. (8).

The function  $R$  is an integral over the steady states across the network, via the derivative of the activation function  $f$ . It is maximal whenever  $\bar{u}_{on,off} = h$ , that is, the closer the equilibrium activities are to the threshold for firing (and thus for producing feedback activity), the higher  $R$  becomes. It may also be seen as the amount of non-linearity in the system. With adaptation, significant variations of the function  $R$  require large input amplitudes. In the context of a static pulse of width  $\Delta$

and amplitude  $I_o$ , Fig. 5 illustrates points in  $(I_o, \epsilon)$  parameter space for which an input-induced Andronov–Hopf bifurcation occurs, i.e. for which  $R(I_o, \epsilon) > R_c$ . It illustrates how the function  $R(I_o, \epsilon)$  behaves according to an input amplitude  $I_o$  and increasing adaptation gain  $\epsilon$ . A diminished input amplitude implies that larger input amplitudes are required to bring the system in regions of parameter space where oscillations are stable

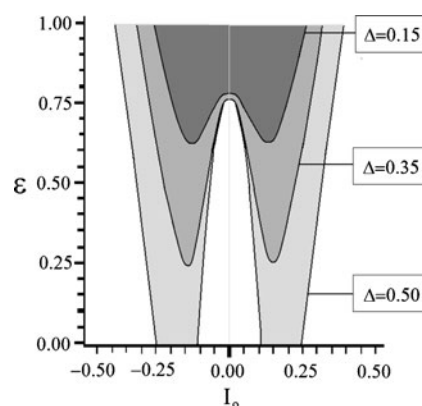


**Fig. 6** Points in  $(I_o, \epsilon)$  parameter space for which  $R(\epsilon) > R_c$  for a static pulse-shaped stimulus of amplitude  $I_o$  and various widths. Pulses of smaller widths only generate rhythmic responses when the adaptation gain is increased. Regions where the limit cycles are stable, plotted in shades of gray, are symmetric with respect to the line  $I_o$ . Parameters are  $a = 1$ ,  $\tau = 2.0$ ,  $\Omega = [0, 1]$ ,  $h = 0.07$  and  $b = 0.8$

(gray regions). But it also implies that once the system reaches those states, they are more robust and remain stable over a larger range of input amplitudes.

Cellular adaptation diminishes the variability of  $R$ . When  $h$  is low, more significant contributions are made by the lateral units to the non-linear connections; this is even more so as the adaptation gain increases. The steady states  $\bar{u}_{on,off}$  of lateral sites are higher for  $\epsilon > 0$  due to less feedback inhibition, and are typically found closer to the activation threshold  $h$ . This results in higher values of the function  $R(I_o, \epsilon)$ : the system remains close to the Andronov–Hopf regime over a larger portion of parameter space because the adaptation disposes the lateral activities to maintain a higher degree of non-linearity. As shown in Fig. 5(a), the minimal amplitude required for global oscillations is smaller for  $\epsilon > 0$  than for  $\epsilon = 0$ . For high values of  $h$ ,

the effect of the adaptation gain on the lateral contributions is negligible, since the reduced contrast causes the function  $R(I_o, \epsilon)$  to be much smaller when  $\epsilon > 0$  than when  $\epsilon = 0$ . This is the case depicted in Fig. 5(b). Nevertheless, the broadening of the amplitude intervals due to  $\epsilon$  makes oscillations more prevalent in a system that incorporates adaptation. This supports previous results on recurrent nets with adaptation, where slow recurrent components were shown to facilitate the genesis of cyclic activity (Crook et al. 1998; Ermentrout et al. 2001; Ly and Ermentrout 2010). We note that whenever the input absolute amplitude increases, the system first enters the Andronov–Hopf regime where global oscillations are stable; but if the input amplitude becomes too high, the oscillations disappear via a reverse Andronov–Hopf bifurcation. This is so because the sub-unit activities are taken to values much higher

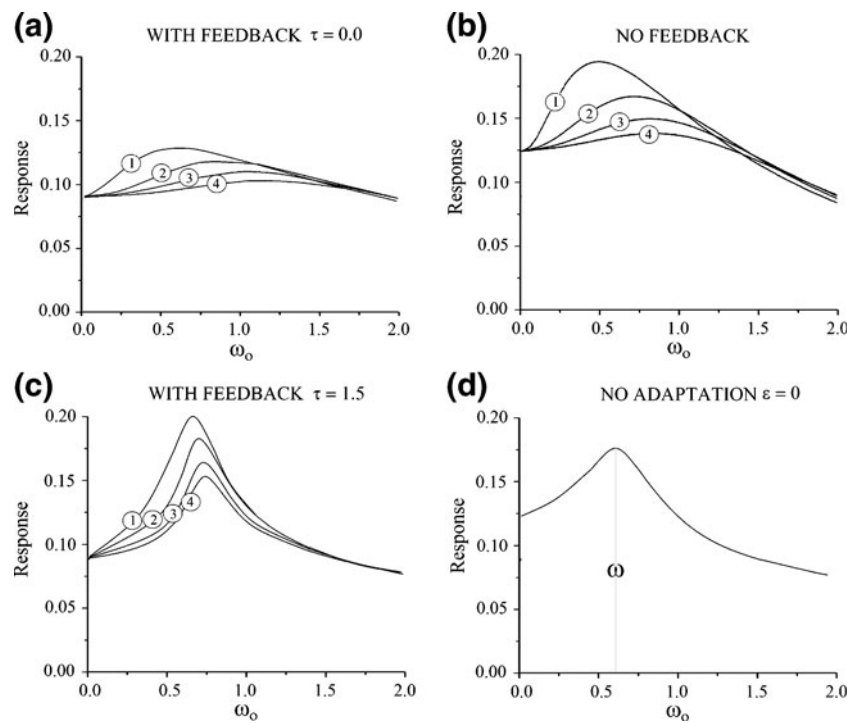


**Fig. 7** Response amplitude of ON cells to a spatially localized pulse sinusoidally modulated in time i.e.  $I(x) = I_o \sin(\omega_o t)$  for  $x \in \Delta$ . The response is defined as the difference between the maximal amplitude of the activity reached by the solutions, and the activity level prior to any stimulus. For each trial, the adaptation time scale is increased, from slow to fast: **1.**  $b = 0.2$ ; **2.**  $b = 0.5$ ; **3.**  $b = 0.8$ ; **4.**  $b = 1.1$ . **(a)** With non-delayed feedback, the response is constant over the range of input frequencies. The system responds maximally to the adaptation intrinsic frequency, while the inhibitory feedback keeps the responses weak. **(b)** Without feedback, the system demonstrates strong resonance

near the adaptation frequencies. The response decreases in amplitude as the adaptation becomes faster. **(c)** When delayed feedback is considered, dominant responses are seen near the Hopf frequency, where the change in adaptation time-scale does not seem to significantly shift the resonances, although the dynamics still become high pass. The delay chosen is  $\tau = 1.5$ . **d)** Without adaptation (i.e.  $\epsilon = 0$ ), the resonance occurs at the Hopf frequency, and the response amplitude is generally larger (even for  $\omega_o = 0.0$ ). Parameters are  $a = 1$ ,  $\Omega = [0, 1]$ ,  $h = 0.1$ ,  $I_o = 0.2$  and  $\Delta = 0.4$ . The adaptation gain was set in panel **(a)–(c)** to  $\epsilon = 0.6$

than the threshold  $h$ , where the feedback  $A$  behaves linearly. The activity of ON and OFF cells is then inhibited sufficiently by the feedback to destroy the oscillations.

Our analytic work assumes that the adaptation rate and gains are equal between ON and OFF populations. However, it has been shown that in the electrosensory system these parameters vary between ON and OFF populations, and also across the various electrosensory spatial maps (Krahe et al. 2008; Mehaffey et al. 2008). In fact, this motivates varying the adaptation rates below in Fig. 7. If the symmetry restriction is relaxed and two distinct adaptation rates  $b_{on}$  and  $b_{off}$  are introduced, the Andronov–Hopf regions of Fig. 5 become non-symmetric with respect to the vertical line  $I_o = 0$ , meaning that the system does not respond evenly to excitatory and inhibitory inputs anymore (not shown). In fact, the sub-population with the slowest adaptation dominates: whenever  $b_{off} < b_{on}$ , a wider range of inhibitory input amplitudes triggers oscillatory activity, i.e. the system becomes more sensitive to inhibitory inputs because OFF cell adaptation is slower. If  $b_{on} < b_{off}$ , the opposite occurs. This effect is amplified with the magnitude of  $|b_{off} - b_{on}|$ .

An interesting consequence of these effects is that the system may now respond to pulses of smaller spatial extent, in a regime where  $h$  is smaller. As the mean value of  $R$  is larger for  $\epsilon > 0$  in this case, input causing small fluctuations in the function  $R$  now becomes a candidate to cause a bifurcation, via either amplitude or width changes. This would not be the case if adaptation were not present, because the mean value of  $R$  would be much smaller. This effect is caused by a smaller amount of inhibition fed back to the sensory layer by the recurrent connections, as the units adapt as well to this steady return current. Figure 6 shows how the regions in  $(I_o, \epsilon)$  space changes as a function of input width. As the width  $\Delta$  diminishes from 0.50 to 0.35, regions of stable oscillatory activity retract towards higher adaptation gains, meaning that adaptation is necessary for those smaller inputs to trigger stable oscillatory solutions. We note that this behavior occurs because of the choice of a small feedback threshold  $h$ .

In Lefebvre et al. (2010), it was shown that if an additional non-delayed inhibitory feedback component is added to Eq. (1), the Andronov–Hopf threshold increases, thus reducing the tendency of the system to undergo oscillatory behavior with respect to spatially localized inputs. In many aspects, an adaptation current like the one considered here plays the same role as an extra instantaneous inhibitory feedback. As Fig. 5 shows, the minimal input amplitude required to generate global oscillations increases, which corroborates

the results presented in Lefebvre et al. (2010) for this particular choice of large threshold values. This seems to contradict the results of Fig. 6, but this is not so. While the main effect of adaptation is to move equilibria in phase space, the non-delayed feedback components considered in Lefebvre et al. (2010) changed the bifurcation threshold considerably, which is not the case here. The oscillations triggered by small pulses as in Fig. 5 are the result of a special choice of  $h$  which brings the system close to the Andronov–Hopf regime.

#### 4 Time-varying inputs

The results presented in the foregoing analysis are based on changes of stability of steady states. However, one of the major role of cellular adaptation is to filter time-varying signals. Fast inputs are likely to significantly increase the cellular activity until the adaptive forces activate. This adaptive component typically acts on the system after the initial, transient response of the cells. As a result, apart from its effect on equilibria, adaptation influences the responses of the system with respect to fast varying signals. As a final part of our overview of adaptation, we outline how the integration of time-dependent inputs varies according to the adaptation parameters  $\epsilon$  and  $b$ . Real sensory signals usually demonstrate a high degree of noise, which can include significant high frequencies. However, studying time-periodic signals may highlight the frequency tuning properties of our model.

The behavior of the solutions with respect to time-dependent inputs might help to understand the role of adaptation and its timing in transient dynamics. In Fig. 7, we plot the response amplitude of the ON cells to a time-periodic signal of frequency  $w_o$  for various adaptation time scales. It is evident that as the adaptation rate constant  $b$  increases, the system filters out lower frequencies, thus acting more like a high-pass filter. When no adaptation is present (Fig. 7(d)), the system's maximal response occurs precisely at the Hopf frequency, as the input resonates with the intrinsic oscillations of the system. If the feedback connections are removed (Fig. 7(b)), the system becomes fully linear and input frequencies generating maximal responses are entirely determined by the amplitude of the solutions of Eq. (3) which are function of  $a, b, w_o$  and  $\epsilon$ . In particular, as adaptation becomes faster (i.e. when  $b$  increases), the response peak is also shifted towards higher input frequencies. A similar behavior occurs in the case with non-delayed feedback (i.e. setting  $\tau = 0$ ), while the system responds maximally at the same

frequencies as in Fig. 7(b), although the amplitudes of the oscillations are significantly smaller.

When both delayed feedback and adaptation (Fig. 7(c)) are considered, the system responds maximally at an input frequency near the Hopf frequency, which corresponds to a mixture of the cases seen in Fig. 7(b) and (d). In this case, the maximal response frequency shift is much less significant, as the system appears to remain closer to the Hopf frequency as  $b$  increases. Increasing the adaptation gain  $\epsilon$  amplifies this effect (not shown).

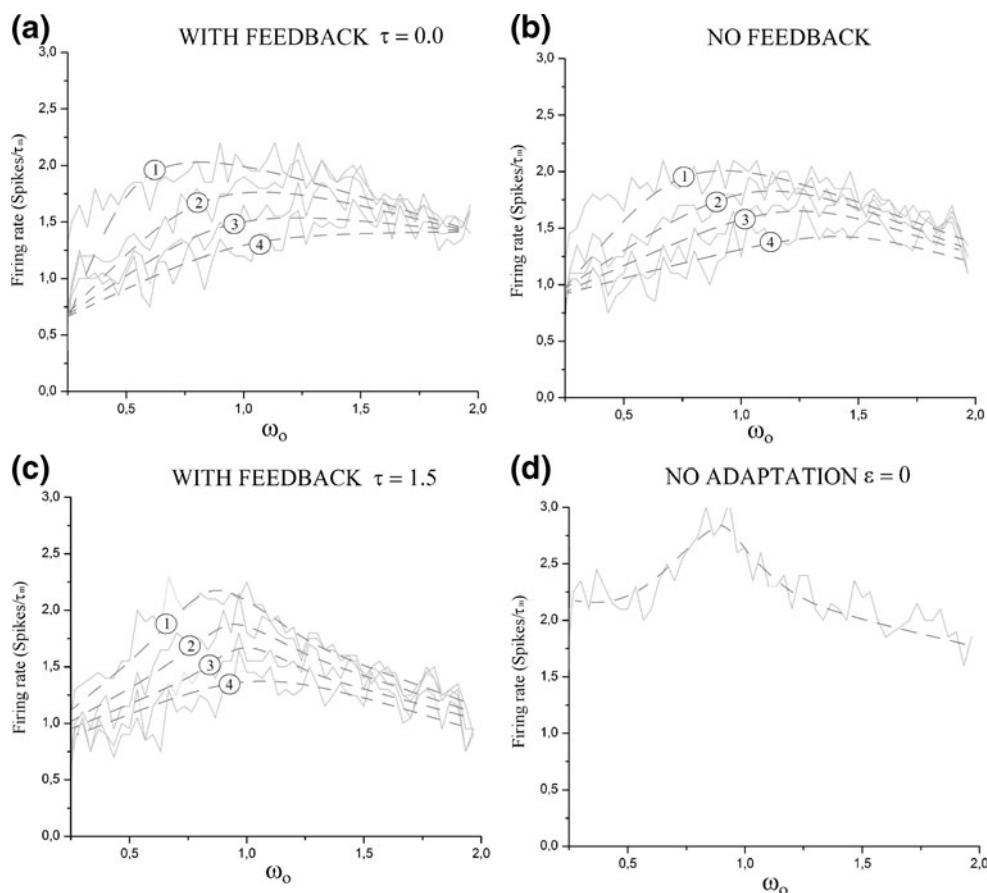
The qualitative shape of the curves shown in Fig. 7 has also been obtained using a noisy Integrate-and-Fire model (LIF) that possesses both global feedback and adaptation, where the architecture is the same as in Eqs. (3) and (4). The goal here is not to perform a thorough comparison of the neural field model dynamics to those of the LIF model—this will be left as part of a future study that will consider more biophysically realistic models of the electrosensory lateral line pyramidal cells, including adaptation, feedback and SK channels. Rather the goal is to show that an LIF description can reproduce the main qualitative features seen in our

neural field model. The evolution of the membrane potential of the  $j$ th LIF neuron, for  $j = 1 \dots N$  obeys

$$\begin{aligned} \frac{dv_j^{on}(t)}{dt} &= -v_j^{on} + g \sum_{t_i} \eta(t_i - \tau) - \epsilon w_j^{on}(t) \\ &\quad + \mu + \xi(t) + I(j, t) \\ \frac{dv_j^{off}(t)}{dt} &= -v_j^{off} + g \sum_{t_i} \eta(t_i - \tau) - \epsilon w_j^{off}(t) \\ &\quad + \mu + \xi(t) - I(j, t) \\ b^{-1} \frac{dw_j^{on}(t)}{dt} &= -w_j^{on}(t) + v_j^{on}(t) \\ b^{-1} \frac{dw_j^{off}(t)}{dt} &= -w_j^{off}(t) + v_j^{off}(t), \end{aligned} \tag{12}$$

with Gaussian white noise  $\xi(t)$  of intensity  $D$ , i.e. the autocorrelation is  $\langle \xi(t)\xi(t') \rangle = 2D\delta(t - t')$ . The feedback gain is denoted by  $g$ . The network contains  $N$  ON cells and  $N$  OFF cells, which receive inputs of the form  $I(j, t)$ . The individual spike times of neurons are denoted by  $t_i$ , and the bias current by  $\mu$ . The synaptic

**Fig. 8** Mean firing rate fluctuations of stimulated ON cells in a noisy Integrate-and-Fire net as in Eq. (12). The input is a spatially localized pulse sinusoidally modulated in time i.e.  $I(x) = I_o \sin(\omega_o t)$  for  $x \in \Delta$ . The plotted firing rates correspond to deviations from the non-stimulated state. As in Fig. 7, the adaptation time scale is increased in each panel: **1.**  $b = 0.2$ ; **2.**  $b = 0.5$ ; **3.**  $b = 0.8$ ; **4.**  $b = 1.1$ . The circuit features are also changed in each panel: **(a)** with non-delayed feedback i.e.  $\tau = 0.0$ ; **(b)** without feedback; **(c)** with delayed feedback i.e.  $\tau = 1.5$ ; and **(d)** without adaptation (i.e.  $\epsilon = 0$ ). In each case, the behavior observed with the neural field model is reproduced qualitatively. Parameters are  $I_o = 1.0$ ,  $\Omega = [0, 1]$ ,  $h = 1.0$ ,  $g = -0.2$ ,  $\mu = 1.05$  and  $\Delta = 0.4$ . The noise has an amplitude  $D = 1.0$ . The adaptation gain was set in panels **(a)–(c)** to  $\epsilon = 1.5$



response function  $\eta$  is an in Eq. (1). The membrane time constant was set to 1, while the refractory period is set to  $\tau_m = 1$ . Here as well,  $b^{-1}$  stands for the adaptation rate and  $\epsilon$  is the adaptation gain.

Numerical results on resonance properties for the LIF with adaptation are shown in Fig. 8. The parameters of the LIF model with ON and OFF cells have been scaled to fit the neural field description, as in Lefebvre et al. (2009). We see that the LIF model qualitatively reproduces the behavior of the resonance when the equivalent parameters are varied. This is particularly the case for the adaptation rate constant. Note that, in the LIF model, the increase in the feedback delay only changes the resonance slightly in comparison to the neural field model. This is likely due to the fact that the LIF includes a feedback kernel which convolves every spike emitted with a smooth function. This kernel already implements an “equivalent” delay, which already causes a resonance similar to the neural field with delay. Nevertheless, the response curves behave as in Fig. 7 to an increase of the adaptation time scale  $b$ , where the processes become more high pass.

## 5 Discussion

In this article, we studied the effects of cellular adaptation on the genesis of oscillatory responses to spatially localized static or time-periodic pulses of varying amplitudes in a recurrent network of ON and OFF cells. Based on previous results, we performed the bifurcation analysis for an Andronov–Hopf bifurcation caused by an external stimulus in an adaptive system, and showed that both the time scale  $b^{-1}$  and gain  $\epsilon$  of the adaptation term modified the instability threshold. The adaptation was shown to decrease the input contrast and the effect of negative feedback, resulting in an increase of steady state activities. It was further shown that for weak values of the adaptation rate and high values of the gain, adaptation enhances the genesis of oscillatory responses to stationary pulses.

Specifically, the results of Section 3 demonstrate that whenever the adaptation rate  $b$  is chosen to be small enough (resulting in slow adaptation dynamics), cyclic solutions are found to be more robust compared to a system that does not adapt at all. In this regime, adaptation causes the Andronov–Hopf threshold to be smaller. This was shown by performing a bifurcation analysis near the fixed points of our model for the case where the adaptation timing and gain are identical for both ON and OFF cells, and by investigating the effect of these on the bifurcation point. A complementary

effect of adaptation may be elucidated by looking at how the activity equilibria behave in the presence of the terms  $w_{on}$  and  $w_{off}$ . Indeed, the adaptation gain affects the input contrast by decreasing the response amplitude of the stimulated units. A direct consequence of this is a wider interval of input amplitudes generating oscillations, making the system more sensitive to inputs of smaller widths. These results point toward a prevalence of oscillatory states generated by sensory stimuli. This result is also consistent with the findings on neural oscillators which show that adaptation enhances the synchronization properties of networks (Crook et al. 1998; Ermentrout et al. 2001), where oscillatory solutions become stable in the presence of adaptation but aren't if feedback alone governs the dynamics (Ly and Ermentrout 2010; Kilpatrick and Bressloff 2010).

However, this conclusion holds only in a regime where the dynamics of  $w_{on,off}$  are slow. In this case, the adaptation components may be seen as an additional source of slow inhibitory feedback (albeit instantaneous rather than delayed), reinforcing the presence of cyclic activity. If the adaptation becomes fast compared to the intrinsic dynamics of the units, the opposite occurs, and global oscillations become more difficult to obtain. This supports the results on a similar model without adaptation, where it was shown that additional non-delayed (and fast) inhibitory feedback components pushed back (i.e. raised) the Andronov–Hopf threshold (Lefebvre et al. 2010).

Adaptation is also involved in the integration of temporal signals. It is thus important to see how this combines with the resonant properties of ON/OFF nets. In Section 4, resonance curves were plotted, in cases with and without feedback. The adaptation component introduces additional resonances in the system. This is apparent by looking at the resonance curves when no feedback is present, or when the feedback delay is chosen to be zero. The Hopf frequency, located at input frequencies where the response amplitude is maximal, depends on the choice of adaptation time scale. The presence of these new frequencies, brought up by two additional complex eigenvalues in Eq. (7), seems to corroborate previous results on frequency tuning regulation properties due to adaptation (Benda and Herz 2003; Mehaffey et al. 2008). Our results are also reproduced by numerical simulations on a network of noisy LIF cells with an equivalent circuitry.

In the perspective of extending the current model, the use of topographic feedback connections would further increase the connection of our work to the electrosensory system. Although an inhibitory spatially diffuse feedback connection does exist between higher nuclei and the sensory layer, other spatially organized

feedback connections branch to the pyramidal cells with glutamatergic as well as gabaergic connections. The topographic feedback in fact brings in a true spatial dimension to the all-to-all connected model. These feedback connections would greatly influence the stability of the activity distributions, especially regarding the presence of spatio-temporal stimuli. Topographic feedback, along with adaptation currents, has been shown to influence the stability of activity patterns and the propagation of oscillations (Folias and Bressloff 2005; Kilpatrick and Bressloff 2010). We thus expect that this will also be the case in our model. It would also be of interest to test whether the dynamics illustrated here differ if ON cells feedback more predominantly to ON cells, and the same for OFF cells. This could lead to predictions about this feedback connectivity.

Further, experimental studies on the weakly electric fish have shown that adaptation time scales vary across the different sensory maps into which the ELL is divided (Krahe et al. 2008). Likewise, the receptive field size of pyramidal cells increases going from central to lateral positions. In this context, it would be interesting to determine how frequency tuning properties of these maps relate to the adaptation time scales when ON and OFF cells are present, and how this tuning depends on receptive field size and topographic feedback. Finally, ON and OFF cells may have different firing rates in the absence of input ( $I(x, t) = 0$ ). This activity difference, when sufficiently strong, can influence the dynamics of recurrent ON/OFF in the absence of adaptation (Lefebvre et al. 2009). The role that it may play in the frequency tuning of cells and oscillation susceptibility of the network with adaptation thus remains to be investigated.

## References

- Bastian, J., Chacron, M. J., & Maler, L. (2002). Receptive field organization determines pyramidal cell stimulus-encoding capability and spatial stimulus selectivity. *Journal of Neuroscience*, *22*, 4577–4590.
- Benda, J., Bethge, M., Hennig, M., Pawelzik, K., & Herz, A. V. M. (2001). Spike-frequency adaptation: Phenomenological model and experimental tests. *Neurocomputing*, *38–40*, 105–110.
- Benda, J., & Herz, A. (2003). A universal model for spike-frequency adaptation. *Neural Computation*, *15*, 2523–2564.
- Benda, J., Longtin, A., & Maler, L. (2005). Spike-frequency adaptation separates transient communication signals from background oscillations. *The Journal of Neuroscience*, *25*, 2312–2321.
- Benda, J., Longtin, A., & Maler, L. (2006). A synchronization-desynchronization code for natural communication signals. *Neuron*, *52*, 347–358.
- Benda, J., Maler, L., & Longtin, A. (2010). Linear versus non-linear signal transmission in integrate-and-fire models with adaptation currents or dynamic thresholds. *Journal of Neurophysiology*. In press.
- Berman, N. J., & Maler, L. (1998). Distal versus proximal inhibitory shaping of feedback excitation in the electrosensory lateral line lobe: Implications for sensory filtering. *Journal of Neurophysiology*, *80*, 3214–3232.
- Berman, N. J., & Maler, L. (1999). Neural architecture of the electrosensory lateral line lobe: Adaptations for coincidence detection, a sensory searchlight and frequency-dependent adaptive filtering. *Journal of Experimental Biology*, *202*, 1243.
- Blomquist, P., Wyller, J., & Einevoll, G. T. (2005). Localized activity patterns in two-population neuronal networks. *Physica D*, *206*, 180.
- Borgers, C., Epstein, S., & Kopell, N. J. (2008). Gamma oscillations mediate stimulus competition and attentional selection in a cortical network model. *Proceedings of the National Academy of Sciences of the United States of America*, *105*, 18023.
- Borgers, C., & Kopell, N. (2003). Synchronization in networks of excitatory and inhibitory neurons with sparse, random connectivity. *Neural Computation*, *15*, 509–538.
- Brandt, S. F., & Wessel, R. (2007). Winner-take-all selection in a neural system with delayed feedback. *Biological Cybernetics*, *97*, 221–228.
- Chacron, M., et al. (2005). Delayed excitatory and inhibitory feedback shape neural information transmission. *Physics Review E*, *72*, 051917.
- Chacron, M., Longtin, A., & Maler, L. (2005). Feedback and feedforward control of frequency tuning to naturalistic stimuli. *Journal of Neuroscience*, *25*, 5521–5532.
- Crook, S., Ermentrout, G. B., & Bower, J. M. (1998). Spike-frequency adaptation affects the synchronization properties of cortical oscillators. *Neural Computation*, *10*, 837–854.
- Curtu, R., & Ermentrout, B. (2004). Pattern formation in a network of excitatory and inhibitory cells with adaptation. *SIAM Journal of Applied Dynamical Systems*, *3*, 191–231.
- Dhamala, M., Jirsa, V. K., & Ding, M. D. (2004). Enhancement of neural synchrony by time delay. *Physical Review Letters*, *92*, 074104.
- Doiron, B., Chacron, M. J., Maler, L., Longtin, A., & Bastian, J. (2003). Inhibitory feedback required for network oscillatory response to communication but not prey stimuli. *Nature*, *421*, 539.
- Doiron, B., Lindner, B., Longtin, A., Bastian, J., & Maler, L. (2004). Oscillatory activity in electrosensory neurons increases with the spatial correlation of the stochastic input stimulus. *Physical Review Letters*, *93*, 4.
- Ermentrout, B., Pascal, M., & Gutkin, B. (2001). The effects of spike frequency adaptation and negative feedback on the synchronization of neural oscillators. *Neural Computation*, *13*, 1285–1310.
- Folias, S. E., & Bressloff, P. (2005). Breathers in two-dimensional neural media. *Physical Review Letters*, *95*, 208107.
- Gabbiani, F. (1996). Coding of time-varying signals in spike trains of linear and half-wave rectifying neurons. *Network Computing in Neural System*, *7*, 61–85.
- Gabbiani, F., & Krapp, H. G. (2006). Spike-frequency adaptation and intrinsic properties of an identified, looming-sensitive neuron. *Journal of Neurophysiology*, *96*, 2951–2962.
- Gollisch, T., & Herz, A. V. M. (2004). Input-driven components of spike-frequency adaptation can be unmasked *in vivo*. *Journal of Neuroscience*, *24*, 7435–7444.

- Gollisch, T., & Meister, M. (2008). Modeling convergent on and off pathways in the early visual system. *Biological Cybernetics*, *99*, 263–278.
- Golomb, D., & Ermentrout, G. B. (2001). Bistability in pulse propagation in networks of excitatory and inhibitory populations. *Physical Review Letters*, *86*, 4179.
- Gray, C. M., & Singer, W. (1989). Stimulus-specific neuronal oscillations in orientation columns of cat visual cortex. *Proceedings of the National Academy of Sciences of the United States of America*, *86*, 1698–1702.
- Kandel, E. R., & Schwarzs, J. H. (1983). *Principles of neural science*. New York: Elsevier.
- Kilpatrick, Z. P., & Bressloff, P. C. (2010). Effects of synaptic depression and adaptation on spatiotemporal dynamics of an excitatory neuronal network. *Physica D*, *239*, 547–560.
- Kim, K. J., & Rieke, F. (2001). Temporal contrast adaptation in the input and output signals of salamander retinal ganglion cells. *Journal of Neuroscience*, *21*, 287–299.
- Kim, K. J., & Rieke, F. (2003). Slow Na<sup>+</sup> inactivation and variance adaptation in salamander retinal ganglion cells. *Journal of Neuroscience*, *23*, 1506–1516.
- Krahe, R., Bastian, J., & Chacron, M. J. (2008). Temporal processing across multiple topographic maps in the electrosensory system. *Journal of Neurophysiology*, *100*, 852–867.
- Laing, C., & Coombes, S. (2006). The importance of different timings of excitatory and inhibitory pathways in neural field models. *Network*, *17*, 151.
- Lefebvre, J., Longtin, A., & LeBlanc, V. G. (2009). Dynamics of driven recurrent networks of on and off cells. *Physics Review E*, *80*, 041912.
- Lefebvre, J., Longtin, A., & LeBlanc, V. G. (2010). Oscillatory response in a sensory network of on and off cells with instantaneous and delayed recurrent connections. *Philosophical Transactions of the Royal Society A: Mathematical, Physical and Engineering Sciences*, *368*, 455–467.
- Liang, Z., & Freed, M. A. (2010). The on pathway rectifies the off pathway of the mammalian retina. *Journal of Neuroscience*, *30*, 5533–5543.
- Lindner, B., Doiron, B., & Longtin, A. (2005). Theory of oscillatory firing induced by spatially correlated noise and delayed inhibitory feedback. *Physics Review E*, *72*, 061919.
- Liu, Y. H., & Wang, X. J. (2001). Spike-frequency adaptation of a generalized leaky integrate-and-fire model neuron. *Journal of Computational Neuroscience*, *10*, 25–45.
- Ly, C., & Ermentrout, G. B. (2010). Analysis of recurrent networks of pulse-coupled noisy neural oscillators. *SIAM Journal of Applied Dynamical Systems*, *9*, 113–137.
- Maler, L., Sas, E., Johnston, S., & Ellis, W. (1991). An atlas of the brain of the electric fish *Apteronotus leptorhynchus*. *Journal of Chemical Neuroanatomy*, *4*, 1–38.
- Marinazzo, D., Kappen, H. J., & Gielen, S. C. A. M. (2007). Input-driven oscillations in networks with excitatory and inhibitory neurons with dynamic synapses. *Neural Computation*, *19*, 1739–1765.
- Mathieson, W. B., & Maler, L. (1988). Morphological and electrophysiological properties of a novel *in vitro* preparation: The electrosensory lateral line lobe brain slice. *Journal of Comparative Physiology A*, *163*, 489–506.
- Mehaffey, W. H., Maler, L., & Turner, R. W. (2008). Intrinsic frequency tuning in ELL pyramidal cells varies across electrosensory maps. *Journal of Neurophysiology*, *99*, 2641–2655.
- Pauluis, Q. (2000). Statistical signs of common inhibitory feedback with delay. *Neural Computation*, *12*, 2513–2518.
- Pauluis, Q., Baker, S. N., & Olivier, E. (1999). Emergent oscillations in a realistic network: The role of inhibition and the effect of the spatiotemporal distribution of the input. *Journal of Computational Neuroscience*, *6*, 27–48.
- Prescott, S. A., et al. (2006). Nonlinear interaction between shunting and adaptation controls a switch between integration and coincidence detection in pyramidal neurons. *Journal of Neuroscience*, *26*, 9084–9097.
- Prescott, S. A., & Sejnowski, T. J. (2008). Spike-rate coding and spike-time coding are affected oppositely by different adaptation mechanisms. *Journal of Neuroscience*, *28*, 13649–13661.
- Robin, D. A., & Royer, F. L. (1987). Auditory temporal processing: Two-tone flutter fusion and a model of temporal integration. *Journal of the Acoustical Society of America*, *82*, 1207.
- Sah, P., & Davies, P. (2000). Calcium-activated potassium currents in mammalian neurons. *Clinical and Experimental Pharmacology and Physiology*, *27*, 657–663.
- Scholl, B., Gao, X., & Wehr, M. (2010). Nonoverlapping sets of synapses drive on responses and off responses in auditory cortex. *Neuron*, *65*, 412–421.
- Sobel, E., & Tank, D. W. (1994). *In vivo* Ca<sup>2+</sup> dynamics in a cricket auditory neuron: An example of chemical computation. *Science*, *263*, 823–826.
- Storm, J. F. (1990). Potassium currents in hippocampal pyramidal cells. *Progress in Brain Research*, *83*, 161–187.
- van Vreeswijk, C., & Hansel, D. (2001). Patterns of synchrony in neural networks with spike adaptation. *Neural Computation*, *13*, 959–992.
- Wang, X. J., Liu, Y., Sanchez-Vives, M. V., & McCormick, D. A. (2003). Adaptation and temporal decorrelation by single neurons in the primary visual cortex. *Journal of Neurophysiology*, *89*, 3279–3293.
- Whittington, M. A., Traub, R. D., & Jeffery's, J. G. R. (1995). Synchronized oscillations in interneuron networks driven by metabotropic glutamate receptor activation. *Nature*, *373*, 612–615.
- Wilson, H. R., & Cowan, J. D. (1972). Excitatory and inhibitory interactions in localized populations of model neurons. *Biophysical Journal*, *12*:1–24.
- Xu, Z., Payne, J. R., & Nelson, M. E. (1996). Logarithmic time course of sensory adaptation in electrosensory afferent nerve fibers in a weakly electric fish. *Journal of Neurophysiology*, *76*, 2020–2032.